

Noncovalent Approach to One-Dimensional Ion Conductors: Enhancement of Ionic Conductivities in Nanostructured Columnar Liquid Crystals

Harutoki Shimura,[†] Masafumi Yoshio,[†] Koji Hoshino,[†] Tomohiro Mukai,[‡] Hiroyuki Ohno,[‡] and Takashi Kato^{*†}

Department of Chemistry and Biotechnology, School of Engineering, The University of Tokyo, Hongo, Bunkyo-ku, Tokyo 113-8656, Japan, and Department of Biotechnology, Tokyo University of Agriculture and Technology, Nakacho, Koganei, Tokyo 184-8588, Japan

Received September 29, 2007; E-mail: kato@chiral.t.u-tokyo.ac.jp

Abstract: Noncovalent design of new liquid-crystalline (LC) columnar assemblies based on an ionic liquid has shown to be useful to achieve anisotropic high ionic conductivities. An equimolar mixture of an ionic liquid, 1-butyl-3-methylimidazolium bromide, and 3-[3,4,5-tri(octyloxy)benzoyloxy]propane-1,2-diol, which is partially miscible with the ionic liquid, exhibits an LC hexagonal columnar phase from -4 to 63 °C. This columnar supramolecular assembly forming the nanostructures shows the one-dimensional (1D) ionic conductivity of 3.9×10^{-3} S cm $^{-1}$ at 50 °C along the column, which is more than 700 times higher than that of the corresponding covalent-type columnar ionic liquid, 1-methyl-3-[3,4,5-tri(octyloxy)benzyl]-imidazolium bromide, which is 5.3×10^{-6} S cm $^{-1}$ at 50 °C. This significant enhancement of the ionic conductivity is attributed to the increase of the mobility of the ionic part.

Introduction

Ionic liquids are liquids composed of organic ions.¹ They form disordered molten states at ambient temperature. As these materials show high ionic conductivities and nonvolatility, they have advantages for electrolytes in lithium ion batteries, dye-sensitized solar cells, and fuel cells.² For further functionalization of ionic liquids, the introduction of ordered nanostructures and supramolecular structures^{3–11} is an important approach. Imidazolium-based compounds are widely used as ionic liquids because of their chemical and electrochemical stability and wider

temperature range to be liquid.¹ The self-organization of LC imidazolium salts has led to the development of low-dimensional ion conductors.^{5,6a–e,7,8} In this case, LC nanostructures that were macroscopically oriented were used. For example, one-dimensional (1D) ion conductors composed of organic molecules have been prepared using columnar LC imidazolium salts.⁷ The molecular design of the materials was chemical modification of imidazolium salts that are normal ionic liquids (Figure 1

[†] The University of Tokyo.

[‡] Tokyo University of Agriculture and Technology.

- (1) (a) Rogers, R. D.; Seddon, K. R. Eds. *Ionic Liquids as Green Solvent: Progress and Prospects*; ACS Symposium Series 856; American Chemical Society: Washington, DC, 2003. (b) Wasserscheid, P.; Keim, W. *Angew. Chem., Int. Ed.* **2000**, *39*, 3772–3789. (c) Rogers, R. D.; Seddon, K. R., Eds. *Ionic Liquids: Industrial Applications for Green Chemistry*; ACS Symposium Series 818; American Chemical Society: Washington, DC, 2002. (d) Forsyth, S. A.; Pringle, J. M.; MacFarlane, D. R. *Aust. J. Chem.* **2004**, *57*, 113–119. (e) Ohno, H. Ed. *Electrochemical Aspects of Ionic Liquids*; John Wiley & Sons: Hoboken, NJ, 2005. (f) Welton, T. *Chem. Rev.* **1999**, *99*, 2071–2083. (g) Ohno, H. *Bull. Chem. Soc. Jpn.* **2006**, *79*, 1665–1680. (h) Bara, J. E.; Gabriel, C. J.; Lessmann, S.; Carlisle, T. K.; Finotello, A.; Gin, D. L.; Noble, R. D. *Ind. Eng. Chem. Res.* **2007**, *46*, 5380–5386.
- (2) (a) Bonhôte, P.; Dias, A. P.; Papageorgiou, N.; Kalyanasundaram, K.; Grätzel, M. *Inorg. Chem.* **1996**, *35*, 1168–1178. (b) Buzzeo, M. C.; Evans, R. G.; Compton, R. G. *ChemPhysChem* **2004**, *5*, 1106–1120. (c) Ito, K.; Nishina, N.; Ohno, H. *Electrochim. Acta* **2000**, *45*, 1295–1298. (d) Wang, P.; Zakeeruddin, S. M.; Moser, J. E.; Humphry-Baker, R.; Grätzel, M. *J. Am. Chem. Soc.* **2004**, *126*, 7164–7165. (e) Yoshizawa, M.; Ohno, H. *Electrochim. Acta* **2001**, *46*, 1723–1728. (f) Washiro, S.; Yoshizawa, M.; Nakajima, H.; Ohno, H. *Polymer* **2004**, *45*, 1577–1582. (g) Susan, M. A.; Kaneko, T.; Noda, A.; Watanabe, M. *J. Am. Chem. Soc.* **2005**, *127*, 4976–4983. (h) Hayamizu, K.; Aihara, Y.; Nakagawa, H.; Nukuda, T.; Price, W. S. *J. Phys. Chem. B* **2004**, *108*, 19527–19532.
- (3) (a) Bowlas, C. J.; Bruce, D. W.; Seddon, K. R. *Chem. Commun.* **1996**, 1625–1626. (b) Gordon, C. M.; Holbrey, J. D.; Kennedy, A. R.; Seddon, K. R. *J. Mater. Chem.* **1998**, *8*, 2627–2636. (c) Holbrey, J. D.; Seddon, K. R. *J. Chem. Soc. Dalton Trans.* **1999**, 2133–2139.
- (4) (a) Lehn, J. M. *Polym. Int.* **2002**, *51*, 825–839. (b) Stupp, S. I.; LeBonheur, V.; Walker, K.; Li, L. S.; Huggins, K. E.; Keser, M.; Amstutz, A. *Science* **1997**, *276*, 384–389. (c) Kato, T.; Mizoshita, N.; Kishimoto, K. *Angew. Chem., Int. Ed.* **2006**, *45*, 38–68. (d) Kato, T. *Science* **2002**, *295*, 2414–2418. (e) Brunsveld, L.; Folmer, B. J. B.; Meijer, E. W.; Sijbesma, R. P. *Chem. Rev.* **2001**, *101*, 4071–4097. (f) Bushey, M. L.; Hwang, A.; Stephens, P. W.; Nuckolls, C. *Angew. Chem., Int. Ed.* **2002**, *41*, 2828–2831. (g) Cowling, S. J.; Hall, A. W.; Goodby, J. W.; Wang, Y.; Gleeson, H. F. *J. Mater. Chem.* **2006**, *16*, 2181–2191. (h) Goodby, J. W.; Mehl, G. H.; Saez, I. M.; Tuffin, R. P.; Mackenzie, G.; Auzely-Velty, R.; Benvegna, T.; Plusquellec, D. *Chem. Commun.* **1998**, 2057–2070. (i) Percec, V.; Glodde, M.; Bera, T. K.; Miura, Y.; Shiyankovskaya, I.; Singer, K. D.; Balagurusamy, V. S. K.; Heiney, P. A.; Schnell, I.; Rapp, A.; Spiess, H. W.; Hudson, S. D.; Duan, H. *Nature* **2002**, *419*, 384–387. (j) Percec, V.; Aqad, E.; Peterca, M.; Imam, M. R.; Glodde, M.; Bera, T. K.; Miura, Y.; Balagurusamy, V. S. K.; Ewbank, P. C.; Würthner, F.; Heiney, P. A. *Chem.—Eur. J.* **2007**, *13*, 3330–3345. (k) McCubbin, J. A.; Tong, X.; Wang, R. Y.; Zhao, Y.; Snieckus, V.; Lemieux, R. P. *J. Am. Chem. Soc.* **2004**, *126*, 1161–1167. (l) Gin, D. L.; Lu, X.; Nemade, P. R.; Pecinovsky, C. S.; Xu, Y.; Zhou, M. *Adv. Funct. Mater.* **2006**, *16*, 865–878. (m) Iyer, P. K.; Beck, J. B.; Weder, C.; Rowan, S. J. *Chem. Commun.* **2005**, 319–321. (n) Camerel, F.; Bonardi, L.; Ulrich, G.; Charbonniere, L.; Donnio, B.; Bourgogne, C.; Guillon, D.; Retailleau, P.; Ziessel, R. *Chem. Mater.* **2006**, *18*, 5009–5021. (o) Xu, B.; Swager, T. M. *J. Am. Chem. Soc.* **1995**, *117*, 5011–5012. (p) Barberá, J.; Puig, L.; Romero, P.; Serrano, J. L.; Sierra, T. *J. Am. Chem. Soc.* **2006**, *128*, 4487–4492. (q) Kanie, K.; Nishii, M.; Yasuda, T.; Taki, T.; Ujiie, S.; Kato, T. *J. Mater. Chem.* **2001**, *11*, 2875–2886. (r) Kato, T.; Matsuoka, T.; Nishii, M.; Kamikawa, Y.; Kanie, K.; Nishimura, T.; Yashima, E.; Ujiie, S. *Angew. Chem., Int. Ed.* **2004**, *43*, 1969–1972. (s) Kato, T.; Fréchet, J. M. J. *Macromol. Symp.* **1995**, *98*, 311–326. (t) Kato, T.; Fréchet, J. M. J. *Liq. Cryst.* **2006**, *33*, 1429–1433.
- (5) (a) Yoshio, M.; Mukai, T.; Kanie, K.; Yoshizawa, M.; Ohno, H.; Kato, T. *Adv. Mater.* **2002**, *14*, 351–354. (b) Yoshio, M.; Kato, T.; Mukai, T.; Yoshizawa, M.; Ohno, H. *Mol. Cryst. Liq. Cryst.* **2004**, *413*, 2235–2244.

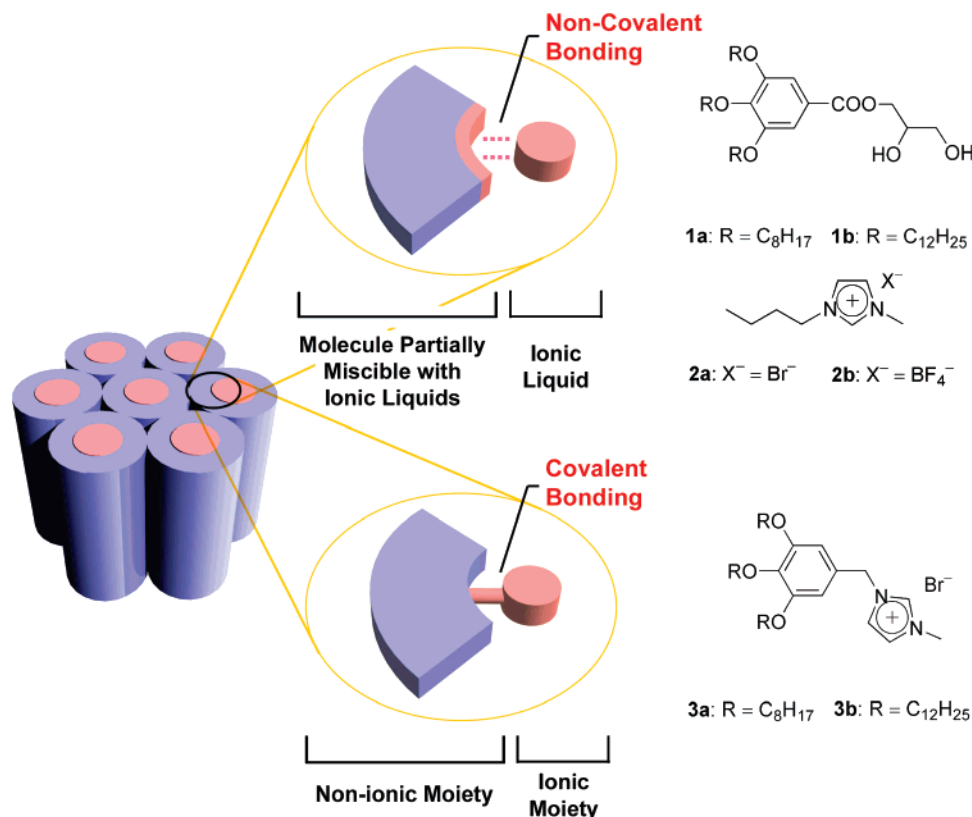


Figure 1. Schematic illustration of the design of the columnar LC molecules and their assemblies for 1D ion conduction: molecular assembly formed through noncovalent bonding between an ionic liquid and a fan-shaped structure-inducing molecule (upper) and a fan-shaped molecule bearing an ionic moiety (lower).

lower). The tri(alkyloxy)phenyl part that has a fan-shaped structure was attached to the ionic moiety to induce self-assembly of the molecule into hexagonal columnar structures due to ionic interactions and nanosegregation between the ionic and nonionic parts. In these nanostructures, ions are transported along the direction of the columnar axis. We have also prepared 1D ion-conductive self-standing films by fixing the aligned columnar LC nanostructures through an *in situ* polymerization technique.⁸ However, their ionic conductivities were still lower

than those required for the practical use (10^{-2} – 10^{-3} S cm⁻¹ at room temperature) as electrolytes for batteries.¹²

Supramolecular and noncovalent materials design has been used to achieve dynamically functional anisotropic materials.⁴ Our materials design in the present study is that we introduce more mobile structures in the LC nanostructures (Figure 1 upper). We have employed noncovalent supramolecular approaches to the materials design. Columnar self-assembled structures have been designed by self-assembly of simpler ionic liquids and fan-shaped (aromatic and aliphatic) molecules that are partially miscible with the salts. If they form nanosegregated columnar structures through self-assembly of these two partially interacting molecular components of ionic liquids and fan-shaped molecules (Figure 1 upper), highly mobile inner columns could be achieved.

Here, we report on 1D ion-conductive columnar liquid crystals formed through self-assembly of ionic liquids and dihydroxy-functionalized fan-shaped molecules. The significant improvement of the conductive properties for the columnar materials has been successfully achieved by the materials design using noncovalent molecular interactions.

- (6) (a) Yoshio, M.; Mukai, T.; Kanie, K.; Yoshizawa, M.; Ohno, H.; Kato, T. *Chem. Lett.* **2002**, 320–321. (b) Hoshino, K.; Yoshio, M.; Mukai, T.; Kishimoto, K.; Ohno, H.; Kato, T. *J. Polym. Sci., Part A: Polym. Chem.* **2003**, *41*, 3486–3492. (c) Mukai, T.; Yoshio, M.; Kato, T.; Ohno, H. *Chem. Lett.* **2004**, 33, 1630–1631. (d) Mukai, T.; Yoshio, M.; Kato, T.; Yoshizawa, M.; Ohno, H. *Chem. Commun.* **2005**, 1333–1335. (e) Mukai, T.; Yoshio, M.; Kato, T.; Ohno, H. *Chem. Lett.* **2005**, 34, 442–443. (f) De Roche, J.; Gordon, C. M.; Imrie, C. T.; Ingram, M. D.; Kennedy, A. R.; Lo Celso, F.; Triolo, A. *Chem. Mater.* **2003**, *15*, 3089–3097. (g) Chen, H.; Kwait, D. C.; Gonen, Z. S.; Weslowski, B. T.; Abdallah, D. J.; Weiss, R. G. *Chem. Mater.* **2002**, *14*, 4063–4072.
- (7) (a) Yoshio, M.; Mukai, T.; Ohno, H.; Kato, T. *J. Am. Chem. Soc.* **2004**, *126*, 994–995. (b) Yoshio, M.; Ichikawa, T.; Shimura, H.; Kagata, T.; Hamasaki, A.; Mukai, T.; Ohno, H.; Kato, T. *Bull. Chem. Soc. Jpn.* **2007**, *80*, 1836–1841. (c) Yoshio, M.; Mukai, T.; Ohno, H.; Kato, T. *ACS Symposium Series 975*; American Chemical Society: Washington, DC, 2007; pp 161–171.
- (8) Yoshio, M.; Kagata, T.; Hoshino, K.; Mukai, T.; Ohno, H.; Kato, T. *J. Am. Chem. Soc.* **2006**, *128*, 5570–5577.
- (9) (a) Lee, C. K.; Huang, H. W.; Lin, I. J. B. *Chem. Commun.* **2000**, 1911–1912. (b) Lin, I. J. B.; Vasam, C. S. *J. Organomet. Chem.* **2005**, *690*, 3498–3512. (c) Bradley, A. E.; Hardacre, C.; Holbrey, J. D.; Johnston, S.; McMath, S. E. J.; Nieuwenhuysen, M. *Chem. Mater.* **2002**, *14*, 629–635. (d) Dobbs, W.; Douce, L.; Allouche, L.; Louati, A.; Malbosc, F.; Welter, R. *New J. Chem.* **2006**, *30*, 528–532.
- (10) (a) Kimizuka, N.; Nakashima, T. *Langmuir* **2001**, *17*, 6759–6761. (b) Nakashima, T.; Kimizuka, N. *Chem. Lett.* **2002**, 1018–1019. (c) Firestone, M. A.; Dzielawa, J. A.; Zapol, P.; Curtiss, L. A.; Seifert, S.; Dietz, M. L. *Langmuir* **2002**, *18*, 7258–7260. (d) Firestone, M. A.; Rickert, P. G.; Seifert, S.; Dietz, M. L. *Inorg. Chim. Acta* **2004**, *357*, 3991–3998. (e) Wang, L. Y.; Chen, X.; Chai, Y. C.; Hao, J. C.; Sui, Z. M.; Zhuang, W. C.; Sun, Z. W. *Chem. Commun.* **2004**, 2840–2841.
- (11) (a) Ohtake, T.; Ogasawara, M.; Ito-Akita, K.; Nishina, N.; Ujiie, S.; Ohno, H.; Kato, T. *Chem. Mater.* **2000**, *12*, 782–789. (b) Ohtake, T.; Takamitsu, Y.; Ito-Akita, K.; Kanie, K.; Yoshizawa, M.; Mukai, T.; Ohno, H.; Kato, T. *Macromolecules* **2000**, *33*, 8109–8111. (c) Kishimoto, K.; Yoshio, M.; Mukai, T.; Yoshizawa, M.; Ohno, H.; Kato, T. *J. Am. Chem. Soc.* **2003**, *125*, 3196–3197. (d) Kishimoto, K.; Suzawa, T.; Yokota, T.; Mukai, T.; Ohno, H.; Kato, T. *J. Am. Chem. Soc.* **2005**, *127*, 15618–15623. (e) Ohtake, T.; Ito, K.; Nishina, N.; Kihara, H.; Ohno, H.; Kato, T. *Polym. J.* **1999**, *31*, 1155–1158. (f) Percec, V.; Johansson, G.; Heck, J. A.; Ungar, G.; Batty, S. V. *J. Chem. Soc., Perkin Trans. 1* **1993**, 1411. (g) Brunsveld, L.; Vekemans, J.; Janssen, H. M.; Meijer, E. W. *Mol. Cryst. Liq. Cryst. Sci. Technol., Sect. A* **1999**, *331*, 2309–2316.
- (12) Murata, K.; Izuchi, S.; Yoshihisa, Y. *Electrochim. Acta* **2000**, *45*, 1501–1508.

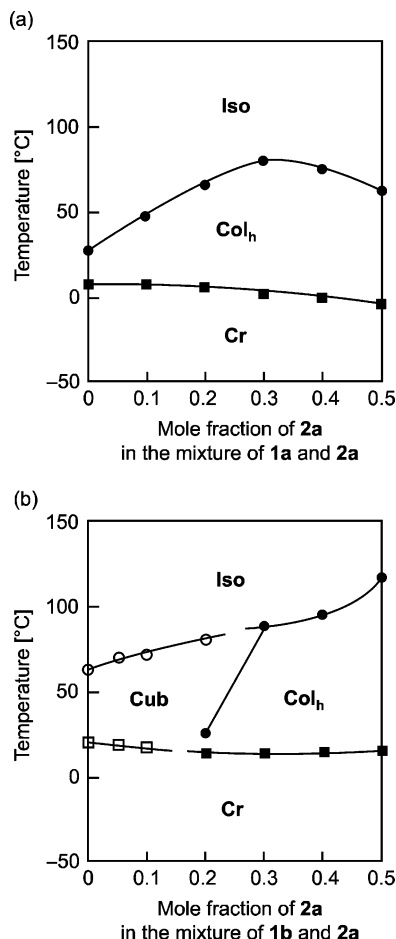


Figure 2. Phase transition behavior for (a) the mixtures of **1a** and **2a** and (b) the mixtures of **1b** and **2a** on heating. Iso, isotropic; Col_h, hexagonal columnar; Cub, micellar cubic; Cr, crystalline.

Results and Discussion

Liquid-Crystalline Properties. We have designed and synthesized fan-shaped molecules **1a,b** having dihydroxy groups at their focal point (Figure 1). They were expected to form self-assembled columnar structures through nanosegregation between ionophilic and lipophilic parts. We reported that hydroxy compounds can form stable hydrogen bonds with imidazolium ions⁵ and imidazoles.¹³ Liquid crystallinity of fan-shaped molecules with polyhydroxy groups has been systematically examined by Tschierske and co-workers.¹⁴ Ionic liquids 1-butyl-3-methylimidazolium salts with bromide anion **2a** and tetrafluoroborate anion **2b** were chosen for supramolecular organization. They are common ionic liquids. LC imidazolium salts **3a,b** have also been synthesized to compare the effects of the noncovalent supramolecular association based on **2a,b** on the ionic conduction and LC behavior of the materials. Compound **1a** exhibits a hexagonal columnar (Col_h) phase from 7 to 27 °C on heating. Figure 2a shows a phase diagram for the mixture of **1a** and **2a** as a function of the mole fraction of **2a** in the mixture. Compound **1a** is miscible with **2a** up to the mole fraction of

0.5 for **2a** in the mixture. The mixing of **1a** and **2a** leads to the thermal stabilization of the Col_h phase compared with the behavior of **1a** itself. The equimolar mixture of **1a** and **2a** shows a Col_h phase from −4 to 63 °C. The mixture of **1a** and **2a** in the molar ratio of 7:3 (**1a/2a** = 7:3) shows the highest columnar–isotropic (Iso) phase transition temperature at 80 °C in all of the mixtures. All of the mixtures keep low melting temperatures around 0 °C. However, further increase of **2a** in the mixture leads to the decrease of Col_h–Iso phase transition temperatures. A macroscopic phase separation into two phases composed of the isotropic liquid and columnar liquid-crystalline phases occurs when the mole fraction of **2a** exceeds 0.5. As for the binary mixtures of **1b** and **2a** (Figure 2b), compound **1b** is also miscible with **2a** up to the mole fraction of 0.5 for **2a** in the mixture. The mixtures having more than the mole fraction of 0.3 for **2a** show a Col_h phase, while **1b** alone and the mixtures containing less than the fraction of 0.2 for **2a** show cubic (Cub) phases. These Cub phases are viscous and optically isotropic under the polarizing optical microscope. The isotropization temperatures increase with the increase of the fraction of **2a** until a fraction of 0.5 is achieved for **2a**. For instance, an equimolar mixture of **1b** and **2a** shows a Col_h phase from 24 to 120 °C on heating. These results suggest that these columnar assemblies are stabilized by the formation of hydrogen bonds between the ions and the hydroxy groups. Similar stabilization of the mesophase by hydrogen bonding and charge transfer interactions has been reported previously.^{4,15}

It is of interest that the mixtures of **1a,b** with **2b** having the BF₄ ion exhibit macrophase separation and they do not form homogeneous LC states although **2a** shows miscibility with **1a** and **1b**. For the supramolecular columnar formation, the ratio of the volumes for ionic and nonionic parts is important. In the case of BF₄, the anion cannot stay in the inner ionic part of the column because of its larger size and weaker interactions. The ionic radius of BF₄ is 0.229 nm, while that of Br is 0.196 nm.

In our previous studies,⁵ we observed that hydroxy-functional rod-shaped LC molecules forming smectic LC structures were miscible with 1-ethyl-3-methylimidazolium tetrafluoroborate. Their layered LC structures having BF₄ anions were stabilized through intermolecular interactions. It is considered that the formation of smectic sheetlike networks is easier than that of the columnar networks. Therefore the nanosegregated smectic phases were stabilized even though ionic interactions based on BF₄ are weaker than those for Br.

Rogers and co-workers reported¹⁶ that imidazolium ionic liquids containing chloride and bromide anions, which are strong hydrogen bond acceptors, solvated cellulose through hydrogen bonding between the hydroxy groups and the anions, whereas ionic liquids with noncoordinating anions BF₄ and PF₆ did not serve as solvents for cellulose. Kimizuka and Nakashima also reported^{10a} that solubility of sugar derivatives in imidazolium ionic liquids decreased when the bromide anion was replaced by hydrophobic anions such as PF₆ and bis(trifluoromethanesulfonyl)imide (TFSI). Moreover, the formation of hydrogen bonds between imidazolium cations and hydroxy groups was

- (13) (a) Kato, T.; Kawakami, T. *Chem. Lett.* **1997**, 211–212. (b) Kato, T. *Struct. Bonding* **2000**, 96, 95–146.
 (14) (a) Borisch, K.; Diele, S.; Göring, P.; Kresse, H.; Tschierske, C. *Angew. Chem., Int. Ed. Engl.* **1997**, 36, 2087–2089. (b) Borisch, K.; Diele, S.; Göring, P.; Kresse, H.; Tschierske, C. *J. Mater. Chem.* **1998**, 8, 529–543. (c) Borisch, K.; Tschierske, C.; Göring, P.; Diele, S. *Chem. Commun.* **1998**, 2711–2712. (d) Borisch, K.; Tschierske, C.; Göring, P.; Diele, S. *Langmuir* **2000**, 16, 6701–6708.

- (15) (a) Kato, T.; Fréchet, J. M. J. *Macromolecules* **1989**, 22, 3818–3819. (b) Ringsdorf, H.; Wüstefeld, R.; Zerta, E.; Ebert, M.; Wendorff, J. H. *Angew. Chem., Int. Ed. Engl.* **1989**, 28, 914–918. (c) Ujiie, S.; Tanaka, Y.; Imura, K. *Chem. Lett.* **1991**, 1037–1040. (d) Kamikawa, Y.; Kato, T. *Org. Lett.* **2006**, 8, 2463–2466.
 (16) Swatoski, R. P.; Spear, S. K.; Holbrey, J. D.; Rogers, R. D. *J. Am. Chem. Soc.* **2002**, 124, 4974–4975.

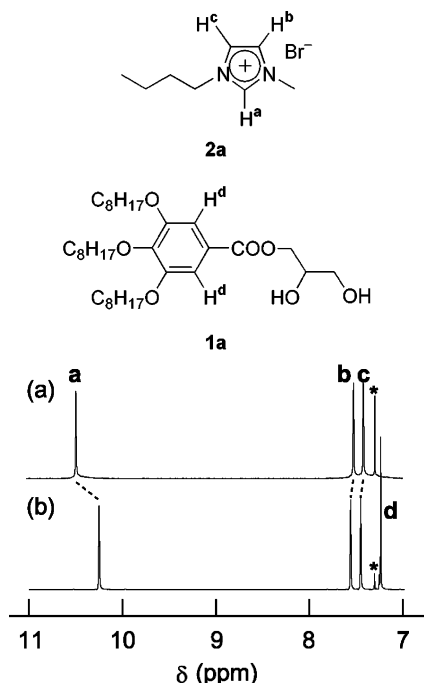


Figure 3. ^1H NMR spectra of (a) **2a** alone and (b) the equimolar mixture of **1a** and **2a** in CDCl_3 (50 mM) at 20 $^\circ\text{C}$. Asterisks denote the proton of CHCl_3 .

clarified by the X-ray crystallographic studies by Rogers et al.¹⁷ The racemic 1-(2-hydroxypropyl)-3-methylimidazolium tetraphenylborate forms a hydrogen-bonded dimer. In this structure, strong and almost linear hydrogen bonds are formed between the acidic hydrogen on C2 of the imidazolium ring and the oxygen atom of the opposing cation.

The interaction between **2a** and **1a** has been confirmed by ^1H NMR experiments (Figure 3). The spectrum for the CDCl_3 solution of **2a** (50 mM) was compared with that of the equimolar mixture of **1a** and **2a** (50 mM). The peak of the proton on C2 of the imidazolium ring for **2a** shows a high-field shift in the presence of **1a** (Figure 3). This change is indicative of the formation of hydrogen bonds between **2a** and **1a**.^{2a} The IR spectra for the mixtures also support the existence of the self-assembled structures (see Supporting Information).

Covalent-type imidazolium salt **3a** (Figure 1) exhibits a Col_h phase from -26 to 180 $^\circ\text{C}$, and **3b** also shows a Col_h phase from 73 to 180 $^\circ\text{C}$. These phase properties were confirmed by microscopic observation and X-ray diffraction studies (see Supporting Information).

The X-ray diffraction measurements for the single components of **1a, b** and their mixtures with **2a** were carried out to examine the structural changes by noncovalent interactions between **2a** and the hydroxy groups of **1a, b**. The X-ray profile for **1a** exhibits the sharp reflections of 2.96 (100), 1.71 (110), 1.48 nm (200) and the broad halo at 0.437 nm, indicating the formation of a disordered Col_h phase ($p6mm$) (see Supporting Information). The intercolumnar distance of **1a** is 3.42 nm. The equimolar complex of **1a** and **2a** exhibits the sharp reflections of 3.77 (100), 2.53 (110), 1.89 nm (200) and the broad halo at 0.428 nm, as shown in Figure 4. The intercolumnar distance for the complex is 4.60 nm. Likewise, all other mixtures of **1a**

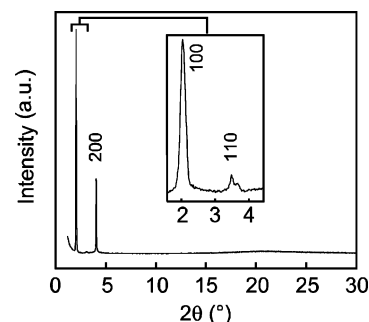


Figure 4. X-ray diffraction pattern of the equimolar mixture of **1a** and **2a** at 30 $^\circ\text{C}$.

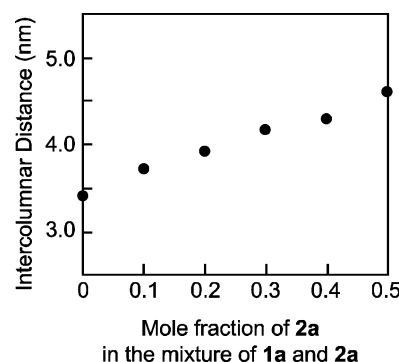


Figure 5. Intercolumnar distance for the self-assembled mixtures composed of **1a** and **2a**.

and **2a** show the d -spacings with the ratio of $1:1/\sqrt{3}:1/2$ in the diffraction spectra, which is typical for the Col_h phase. The intercolumnar distance for the mixtures increases linearly from 3.42 to 4.60 nm with the increase of the mole fraction of **2a** in the mixtures (Figure 5). These results suggest that **2a** is organized into the center of the columnar structures.

Orientation. Uniaxial orientation of the self-organized columnar assemblies has been achieved for these two component systems, which is essential for anisotropic 1D ion conduction. These columns normally prefer to form random orientation on the surface of glassy substrates. To align the columns uniaxially, a shear stress parallel to the surface of the substrate was applied to the columnar materials comprised of the polydomain structures. After shearing the materials, no boundary of the columnar domains was observed under a polarizing microscope. The macroscopic orientation of columns has been confirmed by microscope observation and two-dimensional small-angle X-ray scattering measurements. A split diffraction pattern is observed for the sheared samples, indicating a uniaxial orientation of columns along the direction of shearing (Figure 6).⁸

Ion-Conductive Properties. The columnar LC assemblies composed of equimolar mixtures of **1a, b** and **2a** (**1a/2a** and **1b/2a**) and **3a, b** were homogeneously aligned by mechanical shearing in two directions parallel and perpendicular to the comb-shaped gold electrodes deposited on a glassy substrate. For these samples, ionic conductivities for two directions parallel and perpendicular to the columnar axis have been successfully measured by the alternating current impedance method.^{7,8} We have found that the supramolecular noncovalent ion-conductive LC column of **1a/2a** shows high conductivities that are on the order of $10^{-3} \text{ S cm}^{-1}$ at ambient temperature.

Figure 7 shows ionic conductivities of **1a/2a** and **3a** in the direction parallel (σ_{\parallel}) and perpendicular (σ_{\perp}) to the columnar

(17) Holbrey, J. D.; Turner, M. B.; Reichert, W. M.; Rogers, R. D. *Green Chem.* **2003**, *5*, 731–736.

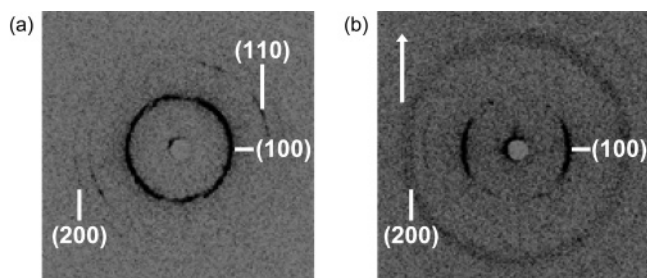


Figure 6. Two-dimensional X-ray scattering images of the equimolar mixture of **1b** and **2a** in the Col_h phase: (a) nonoriented material; (b) uniaxially oriented material. The arrow shows the direction of shearing.

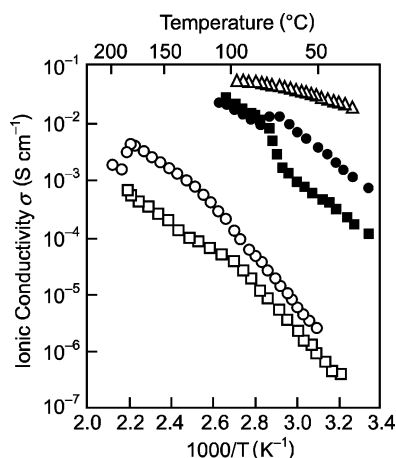


Figure 7. Arrhenius plots of ionic conductivities for **1a/2a** and **3a**, and ionic liquid **2a** alone on heating: (●) parallel and (■) perpendicular to the columnar axis for **1a/2a**; (○) parallel and (□) perpendicular to the columnar axis for **3a**; for isotropic ionic liquid **2a** (Δ).

axis as a function of temperature. The ionic conductivities of **2a** are also given in Figure 7. Although the ionic conductivities ($\sigma_{||}$) of the newly designed complex **1a/2a** forming the Col_h phase are lower than those of **2a** alone that shows the isotropic liquid state, the values of **1a/2a** are in the highest level among those of columnar liquid crystals based on imidazolium salts.^{7,8} For example, complex **1a/2a** shows the $\sigma_{||}$ values of 3.9×10^{-3} S cm⁻¹ at 50 °C and 8.2×10^{-3} S cm⁻¹ at 62 °C. We recently reported on a series of columnar LC imidazolium salts^{7,8} shown in Figure 8. These materials show only the conductivities ($\sigma_{||}$) in the range of 10^{-5} – 10^{-8} S cm⁻¹ at 50 °C. For example, compound **4a**^{7a} shows a value of 9.4×10^{-6} S cm⁻¹ at 50 °C, while compound **5**⁸ exhibits a value of 3.1×10^{-5} S cm⁻¹ at 50 °C. For the conductivities of the materials based on the same anion (Br⁻), the $\sigma_{||}$ value of the complex **1a/2a** at 50 °C becomes 730 times higher than that ($\sigma_{||} = 5.3 \times 10^{-6}$ S cm⁻¹ at 50 °C) of fan-shaped imidazolium salt **3a** prepared in the present study. Compound **3a** must be heated up to 170 °C to achieve the same value of the conductivity as that of **1a/2a** at 50 °C. For **1b/2a**, the $\sigma_{||}$ value of 3.0×10^{-4} S cm⁻¹ is obtained in the Col_h phase at 80 °C. This value of **1b/2a** is 250 times higher than the value of $\sigma_{||} = 1.2 \times 10^{-6}$ S cm⁻¹ at 80 °C for the fan-shaped imidazolium salt **3b** (see Supporting Information). For the noncovalent-type materials, the enhanced mobility of the ionic liquid part in the center of the column should improve the ionic conductivity as we designed. The $\sigma_{||}$ values of **1a/2a** and **3a** are higher than the σ_{\perp} values because the structure-directing lipophilic part acts as the ion-insulating part. No anisotropy is observed when the materials become isotropic liquid states

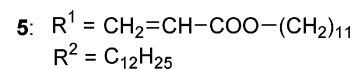
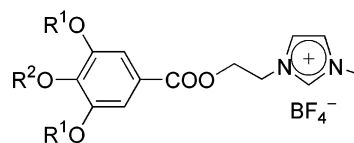
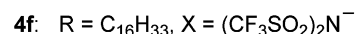
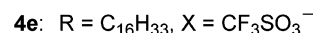
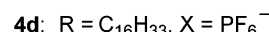
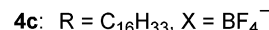
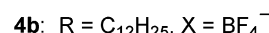
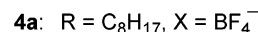
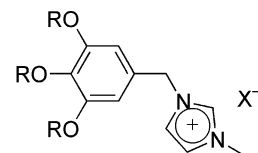


Figure 8. Molecular structures of columnar LC imidazolium derivatives **4a–f** and **5**.⁸

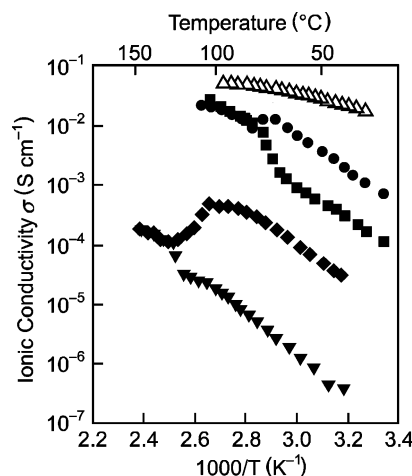


Figure 9. Arrhenius plots of ionic conductivities for **1a/2a**, **1b/2a**, and ionic liquid **2a** alone: (●) parallel and (■) perpendicular to the columnar axis for **1a/2a**; (◆) parallel and (▼) perpendicular to the columnar axis for the mixture based on **1b/2a**; for isotropic ionic liquid **2a** (Δ).

above 63 °C and 180 °C for **1a/2a** and **3a**, respectively. As for **1a/2a**, the anisotropy is observed up to 72 °C because **1a/2a** shows a broader isotropization temperature range. These results indicate that the 1D conducting path is formed in these self-assembled columnar materials.

Figure 9 compares the ionic conductivities of noncovalent-type LC materials **1a/2a** and **1b/2a**. The $\sigma_{||}$ value of 3.9×10^{-3} S cm⁻¹ for **1a/2a** at 50 °C is 79 times higher than that (4.9×10^{-5} S cm⁻¹) of **1b/2a** as a consequence of the lower viscosity of **1a/2a** compared to **1b/2a**. The anisotropy ($\sigma_{||}/\sigma_{\perp}$) of ionic conductivities for **1a/2a** is 7, and that of **1b/2a** is 87 at 50 °C. The higher anisotropy for **1b/2a** is due to the longer dodecyloxy chains of **1b** working as more effective insulating walls to block the leak of ions than the octyloxy chains of **1a**. The values of anisotropy for the noncovalent-type materials show the same

degree as those of the covalent-type materials, depending on the length of alkyloxy chains.

Recently, we reported that the anisotropy of ionic conductivities for the polymer thin films of **5** was about 10^3 , which was in the highest level in the series of our ionic liquid crystal systems. It is interesting to compare the anisotropies of ionic conductivities of columnar ionic liquid crystals with those of electric conductivities of columnar π -conjugated liquid crystals. The anisotropies of electric conductivities of triphenylene^{18a} and tricycloquinazoline^{18b} derivatives were in the range of 10^2 to 10^3 .

Conclusion

New columnar LC assemblies are formed by self-organization of an ionic liquid, 1-butyl-3-methylimidazolium bromide, and mesogenic molecules with hydroxy groups, 3-[3,4,5-tri(alkyloxy)benzoyloxy]propane-1,2-diol, through noncovalent intermolecular interactions. These assemblies are macroscopically aligned by mechanical shearing. They show ionic conductivities on the order of 10^{-3} S cm⁻¹ at ambient temperature which are higher than those of the corresponding covalent-type of columnar LC ionic liquids that are obtained by chemical modification of the ionic liquid. The noncovalent material design shown herein would provide us with low-dimensional ion conductors with a variety of LC nanostructures.^{7,8,19}

Experimental Section

General Procedures. Recycling preparative GPC was conducted with a Japan Analytical Industry LC-908 chromatograph. ¹H and ¹³C NMR spectra were obtained using a JEOL JNM-LA400 at 400 and 100 MHz in CDCl₃, respectively. Chemical shifts of ¹H and ¹³C NMR signals were quoted to internal standard Me₄Si and expressed by chemical shifts in ppm (δ), multiplicity, coupling constant (Hz), and relative intensity. IR measurements were conducted on a JASCO FT/IR-660 Plus on KBr plates. Matrix-assisted laser desorption/ionization time-of-flight (MALDI-TOF) mass spectra were performed on an Applied Biosystems Voyager-DE STR spectrometer. Elemental analyses were carried out with a Perkin-Elmer CHNS/O 2400 apparatus and a Yanaco MT-6 CHN autocorder. Differential scanning calorimetry (DSC) measurements (scanning rate of 10 K min⁻¹) were conducted with a NETZSCH DSC 204 Phoenix differential scanning calorimeter. An Olympus BH-2 optical polarizing microscope equipped with a Mettler FP82 HT hot-stage was used to verify thermal transitions and characterize anisotropic textures. Wide-angle X-ray diffraction (WAXD) patterns were obtained using a Rigaku RINT-2500 diffractometer with Cu K α radiation. Two-dimensional small-angle X-ray scattering (2D SAXS) patterns of the aligned materials were also recorded using an image plate detector (R-AXIS DS3C).

Materials. All chemical reagents and solvents were obtained from commercial sources and used without purification. All reactions were carried out under an argon atmosphere in anhydrous solvents.

Synthesis of 3-[3,4,5-Tri(octyloxy)benzoyloxy]propane-1,2-diol (1a). A solution of 3,4,5-tri(octyloxy)benzoic acid²⁰ (2.03 g, 4.01 mmol), 2,2-dimethyl-1,3-dioxolan-4-methanol (1.35 g, 10.2 mmol), 1-ethyl-3-(3-dimethylaminopropyl)carbodiimide hydrochloride (1.96 g, 10.2 mmol), and 4-dimethylaminopyridine (0.45 g, 3.68 mmol) in dry CH₂Cl₂ (10 mL) was stirred for 3 h at room temperature. The reaction mixture was poured into a sat. NH₄Cl aqueous solution, and the products

were extracted with ethyl acetate. The solvent was evaporated under reduced pressure. The residue was dissolved in wet ethanol (50 mL, containing 5% water). After addition of *p*-toluenesulfonic acid monohydrate (2.30 g, 12.1 mmol), the solution was refluxed for 3 h. After removal of the solvent under reduced pressure, the residue was dissolved in ethyl acetate (50 mL) and washed with water and brine, successively. The resulting organic phase was dried over sodium sulfonate, filtered, and evaporated *in vacuo*. The residue was purified by flash column chromatography on silica gel (eluent: CHCl₃/MeOH = 20/1) followed by GPC to give **1a** (1.80 g, 3.10 mmol, 77%) as a liquid crystal. ¹H NMR (400 MHz, CDCl₃): δ = 7.25 (s, 2 H), 4.46–4.37 (m, 2 H), 4.12–3.92 (m, 7 H), 3.80–3.72 (m, 1 H), 3.72–3.63 (m, 1 H), 2.84 (d, *J* = 4.9 Hz, 1 H), 2.41 (t, *J* = 6.4 Hz, 1 H), 1.90–1.66 (m, 6 H), 1.56–1.16 (m, 30 H), 0.89 (t, *J* = 6.8 Hz, 9H); ¹³C NMR (100 MHz, CDCl₃): δ = 167.0, 152.9, 142.8, 123.9, 108.2, 73.5, 70.4, 69.2, 65.8, 63.3, 31.87, 31.80, 30.3, 29.48, 29.34, 29.32, 29.27, 29.26, 26.05, 26.00, 22.66, 22.65, 14.1. IR (KBr): 3426, 2955, 2926, 2856, 1715, 1587, 1500, 1467, 1430, 1381, 1336, 1254, 1219, 1115, 1058, 1013, 915, 864, 816, 765, 722, 667 cm⁻¹. MS (MALDI) calcd for C₃₄H₆₀O₇: 580.43. Found: 580.74. Elemental analysis calcd for C₃₄H₆₀O₇: C, 70.31; H, 10.41%. Found: C, 70.31; H, 10.65%.

Synthesis of 3-[3,4,5-Tri(dodecyloxy)benzoyloxy]propane-1,2-diol (1b). The compound was prepared from 3,4,5-tri(dodecyloxy)benzoic acid and 2,2-dimethyl-1,3-dioxolan-4-methanol by the method described for **1a** (65%, a translucent solid). ¹H NMR (400 MHz, CDCl₃): δ = 7.25 (s, 2 H), 4.47–4.36 (m, 2 H), 4.13–3.93 (m, 7 H), 3.80–3.72 (m, 1 H), 3.71–3.63 (m, 1 H), 2.80 (d, *J* = 4.9 Hz, 1 H), 2.35 (t, *J* = 6.3 Hz, 1 H), 1.87–1.70 (m, 6 H), 1.56–1.20 (m, 54 H), 0.88 (t, *J* = 6.8 Hz, 9H); ¹³C NMR (100 MHz, CDCl₃): δ = 166.9, 152.8, 142.7, 123.9, 108.1, 73.5, 70.3, 69.2, 65.7, 63.3, 31.89, 31.88, 30.3, 29.71, 29.68, 29.67, 29.65, 29.63, 29.60, 29.5, 29.37, 29.36, 29.33, 29.26, 26.05, 26.00, 22.65, 14.1. IR (KBr): 3394, 2919, 2850, 1712, 1587, 1503, 1469, 1431, 1389, 1338, 1254, 1220, 1120, 859, 762, 721 cm⁻¹. MS (MALDI) calcd for C₄₆H₈₄O₇: 748.62. Found: 748.87. Elemental analysis calcd for C₄₆H₈₄O₇: C, 73.75; H, 11.30%. Found: C, 74.09; H, 11.20%.

Preparation of Ionic Liquid Mixtures: Before making mixtures, the materials were dried under reduced pressure over 80 °C. A CH₂Cl₂ solution of **1a** or **1b** was added to a requisite amount of a CH₂Cl₂ solution of an ionic liquid **2a**^{2a} or **2b**.²¹ The solvent was removed by slow evaporation by using the flow of an argon gas, and the resultant mixture was dried under reduced pressure at 25 °C for 5 h.

Synthesis of 1-Methyl-3-[3,4,5-tri(octyloxy)benzyl]imidazolium Bromide (3a). A mixture of 3,4,5-tris(octyloxy)benzyl bromide²² (0.284 g, 0.511 mmol) and 1-methylimidazole (0.420 g, 5.11 mmol) in a pressure tube (100 mL) equipped with a stirring bar was heated at 80 °C for 10 h with vigorous stirring. The reaction mixture was poured into water and washed. The solid was filtered and then dissolved in chloroform, and the organic phase was separated. The organic phase was washed with a sat. NaCl aqueous solution, dried over anhydrous MgSO₄, filtered through a pad of Celite, and concentrated *in vacuo*. The residue was purified by flash column chromatography on silica gel (eluent: chloroform/methanol = 10/1), followed by recycling GPC, and then recrystallized from acetone to give **3a** (158 mg, 0.247 mmol) in a yield of 48% as a white solid. ¹H NMR (400 MHz, CDCl₃): δ = 10.78 (s, 1H), 7.18 (t, *J* = 1.7 Hz, 1H), 7.16 (t, *J* = 1.7 Hz, 1H), 6.67 (s, 2H), 5.42 (s, 2H), 4.08 (s, 3H), 3.98 (t, *J* = 6.5 Hz, 4H), 3.94 (t, *J* = 6.5 Hz, 2H), 1.85–1.56 (m, 6H), 1.52–1.04 (m, 30H), 0.88 (t, *J* = 7.0 Hz, 9H); ¹³C NMR (100 MHz, CDCl₃): δ = 153.70, 138.74, 137.30, 127.51, 123.08, 121.54, 104.48, 73.37, 69.36, 53.67, 36.71, 31.81, 31.74, 30.23, 29.45, 29.32, 29.29, 29.21, 26.04, 25.98, 22.59, 14.03. IR: 3457, 3378, 3141, 3068, 2925, 2853, 1591, 1559, 1503, 1442, 1388, 1335,

(18) (a) Boden, N.; Bushby, R. J.; Clements, J. J. *Chem. Phys.* **1993**, *98*, 5920–5931. (b) Boden, N.; Borner, R. C.; Bushby, R. J.; Clements, J. J. *Am. Chem. Soc.* **1994**, *116*, 10807–10808.

(19) Ichikawa, T.; Yoshio, M.; Hamasaki, A.; Mukai, T.; Ohno, H.; Kato, T. J. *Am. Chem. Soc.* **2007**, *129*, 10662–10663.

(20) Rowe, K. E.; Bruce, D. W. *J. Mater. Chem.* **1998**, *8*, 331–341.

(21) Nishida, T.; Tashiro, Y.; Yamamoto, M. J. *Fluorine Chem.* **2003**, *120*, 135–141.

(22) Hammond, S. R.; Zhou, W. J.; Gin, D. L.; Avlyanov, J. K. *Liq. Cryst.* **2002**, *29*, 1151–1159.

1247, 1168, 1111, 987, 855, 771, 752, 723, 700, 621 cm^{-1} . MS (MALDI) calcd for $\text{C}_{35}\text{H}_{61}\text{N}_2\text{O}_3^+$: 557.5. Found: 557.5.

Synthesis of 1-Methyl-3-[3,4,5-tri(dodecyloxy)benzyl]imidazolium Bromide (3b). Titled compound was prepared using the same procedure described for **3a**. ^1H NMR (400 MHz, CDCl_3): δ = 10.89 (s, 1H), 7.21 (t, J = 1.7 Hz, 1H), 7.15 (t, J = 1.7 Hz, 1H), 6.65 (s, 2H), 5.42 (s, 2H), 4.08 (s, 3H), 3.96 (t, J = 6.4 Hz, 4H), 3.93 (t, J = 6.4 Hz, 4H), 1.85–1.65 (m, 6H), 1.52–1.11 (m, 54H), 0.88 (t, J = 6.8 Hz, 9H); ^{13}C NMR (100 MHz, CDCl_3): δ = 153.75, 138.83, 138.26, 127.55, 122.85, 121.26, 107.48, 73.40, 69.37, 53.77, 36.61, 31.88, 31.87, 30.27, 29.71, 29.67, 29.64, 29.62, 29.60, 29.55, 29.41, 29.32, 26.08, 26.04, 22.64, 14.08. IR: 3436, 3068, 2919, 2850, 1585, 1560, 1501, 1466, 1389, 1335, 1249, 1170, 1111, 861, 754, 721 cm^{-1} . MS (MALDI) calcd for $\text{C}_{47}\text{H}_{85}\text{N}_2\text{O}_3^+$: 725.7. Found: 725.2.

Measurements of Ionic Conductivities. Temperature dependence of ionic conductivities was measured by the complex impedance method using a Schlumberger Solartron 1260 impedance analyzer (frequency range: 10 Hz–10 MHz, applied voltage: 0.3 V) equipped with a temperature controller.^{6d,7a,23} The heating rate of ionic conductivity measurements was fixed to 3 K min^{-1} from 30 to 150 $^\circ\text{C}$. Ionic conductivities were practically calculated to be the product of $1/R_b$ (Ω^{-1}) times cell constants (cm^{-1}) for comb-shaped gold electrodes, which were calibrated with KCl aqueous solution (1.00 mmol L^{-1}) as a standard conductive solution. The impedance data (Z) were modeled as a connection of two RC circuits in series.

(23) Macdonald, J. R. *Impedance Spectroscopy Emphasizing Solid Materials and Systems*; John Wiley & Sons: New York, 1987.

Acknowledgment. We would like to thank Dr. T. Nishimura for helpful discussions. This study was partially supported by Grant-in-Aid for Scientific Research (A) (No. 19205017) (T.K.) from the Japan Society for the Promotion of Science (JSPS) and Grant-in-Aid for the Global COE Program for Chemistry Innovation through Cooperation of Science and Engineering (T.K.). H.S. is thankful for financial support from JSPS Research Fellowships for Young Scientists.

Supporting Information Available: X-ray diffraction spectra of **1a** in the Col_h phase, **1b** in the Cub phase, the equimolar mixture of **1b** and **2a** in the Col_h phase, **3a** in the Col_h phase, and **3b** in the Col_h phase; ^1H NMR spectra of **2a** alone and the equimolar mixture of **1a** and **2a** in CDCl_3 ; Arrhenius plots of ionic conductivities for **3b**; analytical and spectral characterization data of **3a** and **3b**; an example of the impedance spectrum for the equimolar mixture of **1a** and **2a**; IR spectra of **1a** and the equimolar mixture of **1a** and **2a**; and DSC thermograms and polarized optical microscopic images of **1a**, the equimolar mixture of **1a** and **2a**, **1b**, and the equimolar mixture of **1b** and **2a**. This material is available free of charge via the Internet at <http://pubs.acs.org>.

JA0775220